Nat Hazards
DOI 10.1007/s11069-010-9640-4

ORIGINAL PAPER

Assimilation of Indian radar data with ADAS and 3DVAR techniques for simulation of a small-scale tropical cyclone using ARPS model

Kuldeep Srivastava · Jidong Gao · Keith Brewster · S. K. Roy Bhowmik · Ming Xue · Ranu Gadi

Received: 22 February 2008 / Accepted: 3 October 2010

Abstract The center for Analysis and Prediction of Storms (CAPS) has developed a radar data assimilation system. The system consists of several principal components: (1) a program that quality-controls and remaps (or super-ob) radar data to the analysis grid, (2) a Bratseth analysis method (ADAS), or a 3DVAR method for analyzing all the data except for clouds and precipitation, (3) a cloud and hydrometer analysis package that applies diabetic adjustments to the temperature field, and (4) a non-hydrostatic forecast model named ARPS. In this study, the system is applied to a small cyclone named OGNI, which formed over Bay of Bengal, India during the last week of October 2006. Three experiments are carried out to test the impact of the radar data from Chennai, India. These experiments include (1) using NCEP GFS data to initialize the ARPS model (2) using initial and boundary condition produced from the ADAS and the cloud analysis, (3) using initial and boundary condition produced from the 3DVAR and cloud analysis. The inter-comparison of results reveals that the experiment with the 3DVAR assimilation technique produces more realistic forecast to capture the genesis, structure, and northward movement of the cyclone in the short-range time scale.

Keywords Assimilation of Doppler weather radar data · Small scale cyclone · ARPS · ADAS · 3DVAR

K. Srivastava (✉) · S. K. Roy Bhowmik
India Meteorological Department, NWP Center, Mausam Bhawan, Lodi Road, New Delhi 110003, India
e-mail: kuldeep.nhac@gmail.com

J. Gao · K. Brewster · M. Xue
Center for Analysis and Prediction of Storm, Oklahoma University, Oklahoma, USA

R. Gadi
Indira Gandhi Institute of Technology, Guru Gobind Singh Indraprastha University, Kashmere Gate, New Delhi 110006, India

1 Introduction

The development of high-resolution non-hydrostatic models, the rapid increase of computer power and availability of Doppler radar Data are making great improvement in the prediction of thunderstorms and cyclones. To be successful, a high-resolution prediction system must use all available observations, including Doppler radar data, satellite data, traditional sounding, and surface data in a data assimilation system. Such an assimilation system must produce a balance state that can provide relatively noise-free initial conditions and also contain the hydrometers and latent heating effects that eliminate the need for spinning up mesoscale and storm-scale motion during the initial periods of forecast. The center for Analysis and Prediction of Storms (CAPS), at the University of Oklahoma developed Advance Regional Prediction System (ARPS). It consists of two advanced techniques of data assimilation, namely (a) ARPS Data Assimilation system (ADAS) with a cloud analysis scheme and (b) Three-dimensional variational (3DVAR) technique. The prediction system includes three principal components: (1) programs to remap and super-ob the radar and satellite data to the analysis grid, (2) two alternate (optional) data assimilation system—ADAS with cloud analysis scheme and 3DVAR with cloud analysis scheme and (3) a non-hydrostatic forecast model. It is a comprehensive multi-scale prediction system. The numerical prediction component of the ARPS is a three-dimensional, non-hydrostatic compressible model formulated in generalized terrain following co-ordinates. It contains a comprehensive physics package (Xue et al. 2003)

Radar observations from offshore radar sites provide useful information about the mesoscale structure of tropical cyclone around a landfall. It has been a challenging task to ingest radial wind and reflectivity observations of Indian DWR in the assimilation cycle of a numerical model. Realizing the importance of DWR data in mesoscale NWP modeling, Abhilash et al. (2007) attempted to study the impact of retrieved wind fields from single Indian Doppler radar (Kolkata) for simulation of pre-monsoon convective events over India by MM5 model using 3DVAR data assimilation technique. Wind fields derived from DWR radial wind applying Uniform Wind Technique (UWT) are used in the assimilation cycle of MM5 model. The limitation of the UWT technique is that, due to the simple spatial dependence assumed for the wind field, this technique fails when the wind field is complex (Waldteufel and Corbin 1979). Very recently, Srivastava et al. (2010) carried out study on the assimilation of Indian DWR radial wind and reflectivity observations applying ADAS technique into ARPS model for the convective events over Indian region.

During 29–30 October 2006, Andhra coast of India was hit by a cyclone named as "Ogni". It caused widespread rainfall with scattered heavy to very heavy falls and isolated extremely heavy falls over coastal Andhra Pradesh leading to flood over the region. This provided a unique opportunity to study the impact of DWR observations of Chennai (lat. 13.0° N and long. 80.0° E) with the use of ARPS model to simulate mesoscale convective features which led to inland flooding.

The main interest of this study is to make an inter-comparison of the performance of ADAS and 3DVAR data assimilation techniques, ingesting radial wind and reflectivity observations from an offshore radar site of India (Chennai) with the use of ARPS (version 5.2.5) at 9 km horizontal resolution and to demonstrate its impact on the analysis and forecast for simulation of mesoscale convective features in presence of the Bay of Bengal land-falling cyclone of 29–30 October 2006.

Current assimilation techniques (ADAS and 3DVAR) of ARPS are described in Sect. 2. A brief description of the cyclone Ogni is given in Sect. 3. Section 4 deals with the data sources and design of experiments, results are discussed in Sect. 5, and finally conclusions are summarized in Sect. 6.

2 The data assimilation system

2.1 Processing of the radar data

The data from Chennai radar are brought to a common resolution by remapping the polar coordinate data to the Cartesian terrain-following model grid. This is accomplished by a least squares fit to a local polynomial function that is quadratic in the horizontal and linear in the vertical:

$$A = a_0 + a_1x + a_2x^2 + a_3y + a_4y^2 + a_5xy + a_6z$$

where A is the analyzed variable and a_i are the polynomial coefficients. To avoid any unnatural extrapolation, the result is constrained within the range of data that go into the least squares calculation. At grid resolutions of one to few kilometers, this process performs thinning of radar data by smoothing at close range from the radar, but acts as an interpolator at longer ranges from the radar. The same remapping method is applied to the reflectivity and radial velocity.

2.2 Cloud analysis

The initial foundation of the cloud analysis system was the original cloud analysis of Albers et al. 1996, with adaptation to a general terrain following grid and other enhancements as described by Zhang et al. 1998 and further refinements by Brewster (1996, 2002), Brewster et al. 2003 and Hu et al. (2005a, b). Rules are used to combine the surface observations of cloud layers with satellite measurements of cloud top information, radar data, and thermodynamic information from the three-dimensional analysis.

Cloud Analysis procedure is used to assimilate reflectivity data in ARPS Model. Reflectivity data is used to adjust moisture and temperature in precipitation regions. The radar reflectivity and thermodynamics are used to solve for the hydrometeor mixing ratios.

The analyzed temperature is used to diagnosis of precipitation area. Direct replacement of the background hydrometeors is done in areas where observed reflectivity is greater than a prescribed threshold (typically 10 dBZ). Precipitation is removed from the background in areas having reflectivity less than the precipitation threshold (within the radar volume coverage).

An important aspect to building and maintaining thunderstorm updrafts in a non-hydrostatic model is the inclusion of the effect of latent heat release due to condensation processes in the updraft regions.

A moist adiabatic ascent from the analyzed cloud base with entrainment is calculated, and any excess in this temperature over the analyzed temperature is then added to the analyzed value.

2.3 ADAS technique

The ARPS Data Analysis System (ADAS) (Brewster 1996) uses a successive correction scheme, known as the Bratseth method (Bratseth 1986) and includes radial velocity adjustment. As in the Optimum Interpolation (OI) method, here also correlations among the data must be specified. Typically, the correlations are a function of spatial distance. In ADAS, the correlation, ρ, as a function of horizontal spatial separation is modeled as a Gaussian:

$$\rho_{\mathrm{ij}} = \exp\left(-\left|r_{\mathrm{ij}}\right|^2 / R^2\right)$$

where r_{ij}, j is the displacement between two locations and R is the correlation distance factor. The total correlation is also affected by separation in the vertical. ADAS allows the vertical correlation to be specified as a function of height separation, z

$$\rho_{\Delta \mathrm{z}} = \exp\left(-\Delta Z^2 / R_{\mathrm{z}}^2\right)$$

2.4 3DVAR technique

The 3DVAR analysis method developed for the ARPS model, including dynamic constraints appropriate for storm-scale analysis, is documented in Gao et al. (2002, 2004). The analysis variables contain the three wind components (u, v, and w), potential temperature (θ), pressure (p), and water vapor mixing ratio (q_v). In the current system, the cross-correlations between variables are not included in the background error covariance. The background error correlations for single control variables are modeled by a recursive spatial filter. The observation errors are assumed to be uncorrelated; hence, observation error covariance is a diagonal matrix, and its diagonal elements are specified according to the estimated observation errors.

One unique feature of the ARPS 3DVAR is that multiple analysis passes can be used to analyze different data types with different filter scales to account for the variations in the observation spacing among different data sources.

The main advantage of variational method (3DVAR), over classical data assimilation methods (OI, such as ADAS) is the feasibility of assimilating directly the observed parameters (radial wind and reflectivity) at any given time and space location. Variational assimilation is based on the optimal control theory and the adjoint formulation. Using data directly at observation location avoids an interpolation step, and thus is more beneficial then using quantities derived from the raw observations. Extra processing of data often causes source of errors in addition to the observation errors. The 3DVAR techniques include a mass divergence constraint for coupling the wind components. In fact, ADAS being able to converge to an OI scheme which in turn can be made equivalent to a 3DVAR when only conventional data are involved. The full advantage of 3DVAR scheme will not be realized until indirect observations are involved and proper estimates of the background and observational error correlations are used.

3 The tropical cyclone "Ogni"

During 29–30 October 2006, Andhra coast of India was hit by a cyclone named as "Ogni". It caused widespread rainfall with scattered heavy to very heavy falls and isolated extremely heavy falls over coastal Andhra Pradesh leading to flood over the region. As a result, there were 24 human deaths and heavy loss of property. The area of influence of the Cyclone "Ogni" is shown in Fig. 1. This cyclonic storm was very unique in its nature as it had a very small core (100 km diameter) and short lived (18 h). It moved nearly northward

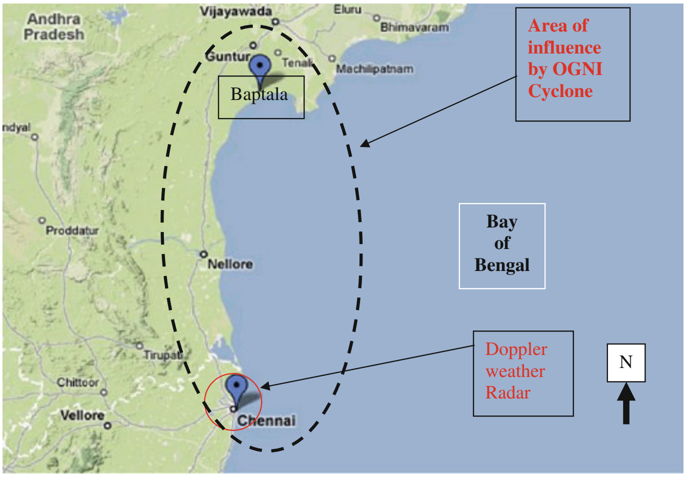

Fig. 1 Study zone for cyclone OGNI of October 2006, *green* area (land) and *blue* area (sea)

over the Bay of Bengal along the coast and weakened into a deep depression before landfall. The system was mainly detected and tracked by Doppler Weather Radar. According to DWR observation at Chennai, the vortex was first noticed in radar scope around 0800 UTC of 28 October. As it was located very close to the coast, it did not get enough Sea travel to attain higher intensity. Radar picture taken by DWR Chennai at 0548 UTC of 29 October is shown in Fig 2. The DWR observation (reflectivity) of Chennai could distinctly capture the vortex in radar scope. Figure 3 displays Indian satellite (KALPANA I) imageries at 0600 UTC of 29 October 2009. The organization of mesoscale convection over the region is clearly depicted. The observed track of the system as reported by India Meteorological Department is given in Fig. 4. The system was moving parallel to the coast, before the landfall.

According to the report documented by Hatwar et al. 2008, a low-pressure area formed over west-central Bay of Bengal off Andhra Pradesh coast in the evening of 28 October 2006. It intensified into a depression and lay centered near lat. 14° N/Long. 80.5° E in the morning of 29. While moving slowly in a northerly direction, it intensified into a deep depression and lay centered near lat. 15° N/80.5° E in the afternoon of the same day. The system further intensified into a cyclonic storm in the evening of 29 October. The system moved slightly northward, and the movement of the system was very slow till the morning of 30 October. It lay centered near lat.19.5° N/long. 83.5° E at 0000 UTC of October 30, 2006. The cyclonic storm moved northwestward and crossed the coast as deep depression around noon of October 30, 2006. After crossing the coast, the system weakened into a depression in the afternoon of same day. The depression further weakened into a low-pressure area over north Andhra Pradesh and adjoining areas in the evening of October 30, 2006. As the system was a small core system, the coastal winds at lower levels were not very strong with wind speed being 20 knots at 850 hPa level at 00 UTC of 28 October. However, the coastal winds suggested gradual intensification of the system from 0000 UTC to 1200 UTC of 29 October and weakening of the system from 0000 UTC of 30 October. However, associated cyclonic circulation (in the operational synoptic weather chart) extended up to mid-troposphere level till morning of 30 October. The steering wind at 200 hPa level at 0000 UTC of 29 October suggested quasi-stationary slow northward

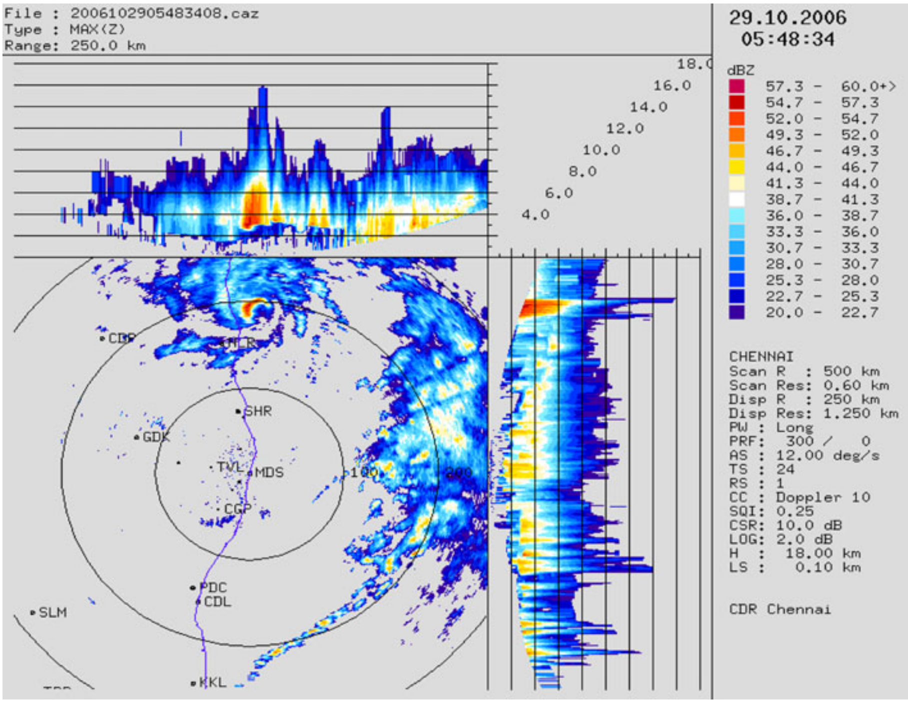

Fig. 2 Radar picture taken by DWR Chennai at 05.48 UTC of 29 October

movement, as it lay close to the ridge line at 200 hPa. The system remained practically stationary or very slow movement at nearly northerly direction throughout its life, covering 135 km in 24 h.

4 Data sources and design of experiments

In the present study, impact of DWR data of Chennai (lat. 13° N, long. 80° E) has been examined in the ARPS (version 5.2.9) data assimilation and forecast at the horizontal resolution of 9 km The scan strategy of 10-min scan was applied to obtain DWR observations. This scan strategy was optimized, taking into account the limitations of the radar hardware and the meteorological requirement of sampling frequency for convective events over the Indian region (Sen Roy et al. 2010). For quality control of these raw data before ingesting into the assimilation system of ARPS, application software (Lakshmanan et al. 2006) called "Warning Decision Software Integrated Information (WDSSII)" is used.

The model domain selected for this study is shown in the Fig 5. Background and boundary conditions are obtained from the National Centre for Environmental Prediction Global Forecast System (NCEP GFS) at the resolution of 1° × 1° lat/long. The NCEP GFS fields are interpolated at 9 km resolution. For experiments, model domain is at 9 km horizontal resolution with 100 × 100 grid points in X and Y direction. This domain covers an area of 900 × 900 km with Chennai located at the center (Fig. 5). The vertical grid stretched from surface to model top, which is located at about 15 km height, at a vertical resolution of 400 m.

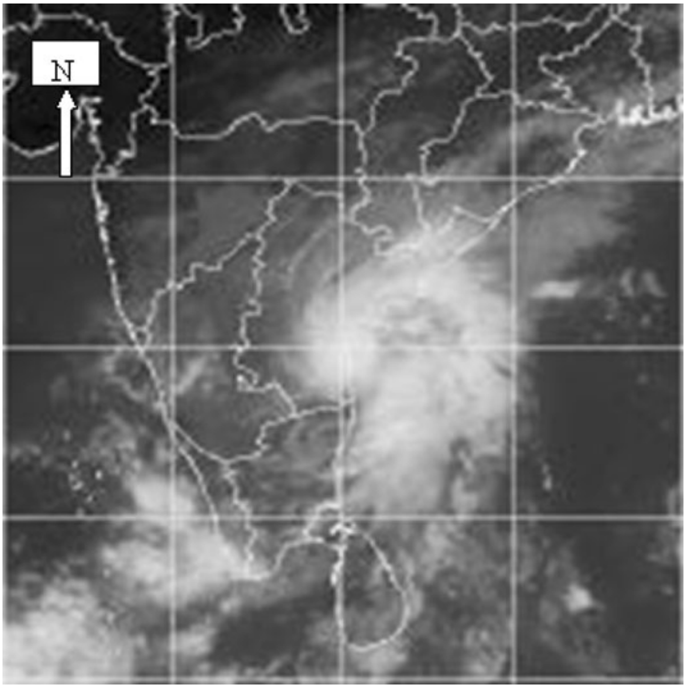

Fig. 3 Indian satellite (KALPANA I) imageries at 0600 UTC of 29 October 2009

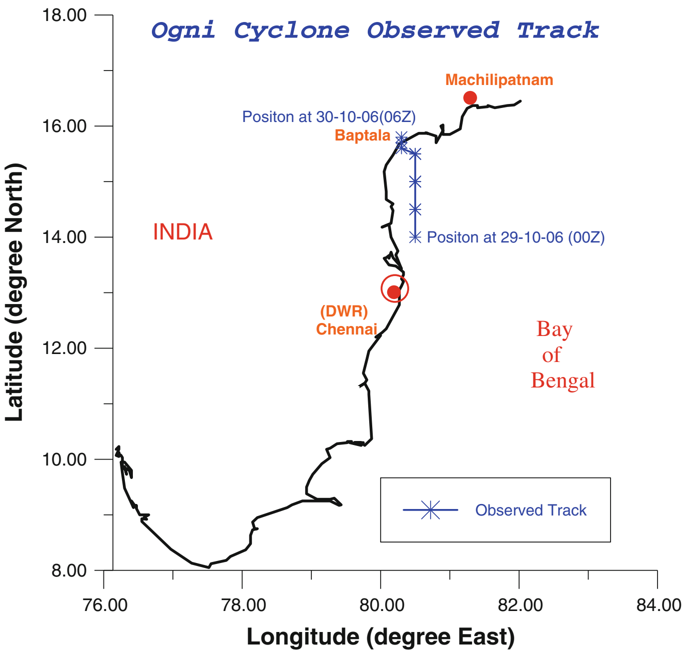

Fig. 4 The observed track of Ogni cyclone

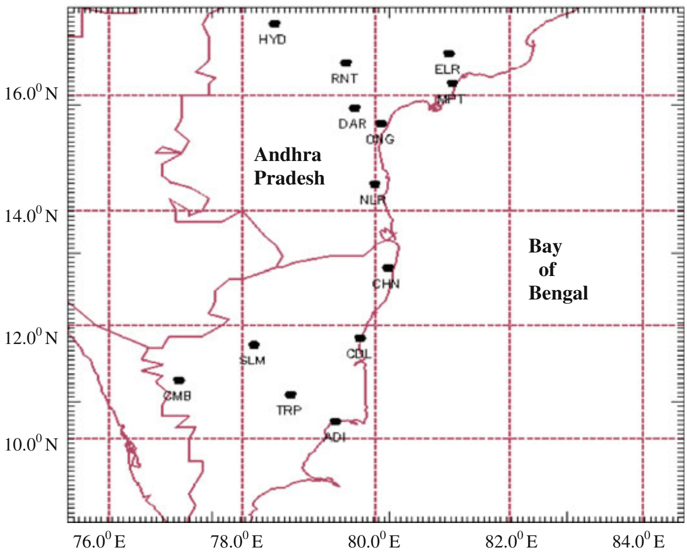

Fig. 5 Model domain for Ogni cyclone

Three sets of numerical experiments are conducted (Table 1). In the first experiment (termed as "control" run), the model is run using National Centre for Environmental Prediction Global Forecast System (NCEP GFS) data (without ingesting radar data) to initialize the ARPS model. In the second experiment (termed as "dwr_ad" run), the model is run using NCEP GFS as the first guess to generate initial field from the assimilation of radar data of Chennai applying ADAS and the cloud analysis scheme. In the third experiment (termed as "dwr_3d" run), the initial condition produced from 3 DVAR with the assimilation of radar data of Chennai and NCEP GFS as the first guess. NCEP GFS forecast fields are used as the boundary condition in these experiments.

The main difference in control run and dwr_ad (or dwr_3d) is that in control run only GFS model forecast is used as the initial and boundary condition. While in dwr_ad (or dwr_3d) experiments, DWR observations (both radial wind and reflectivity) are assimilated along with GFS forecast as the first guess. The main difference between the two assimilation techniques is that ADAS uses statistical optimum interpolation technique (based on successive correction method), while 3DVAR uses variational method (based on control theory for minimization of cost function). In the experiment dwr_ad, radial velocity data are analyzed using ADAS, and reflectivity data are used through the cloud analysis procedure. Half hourly intermittent assimilation cycles are performed within 3-h-long assimilation window from 0000 UTC to 0300 UTC. The life cycle used for the IAU

Table 1 Design of experiments

S. no.	Name of experiment	Type of data assimilated	Technique used for assimilation
1	Control run	No data	–
2	Dwr_ad	DWR (radial velocity and reflectivity)	Successive correction technique
3	Dwr_3d	DWR (radial velocity and reflectivity)	3D variational technique

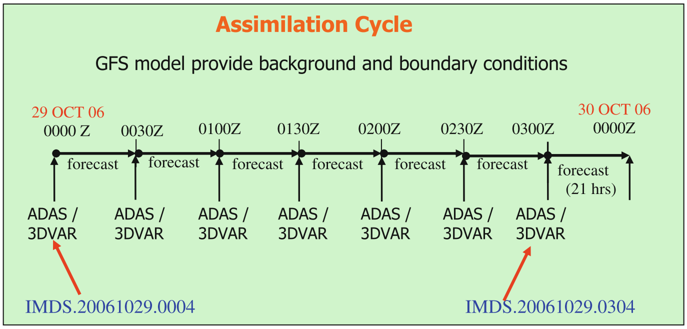

Fig. 6 Thirty minutes data assimilation cycle

assimilation window is 30 min. Figure 6 shows the 3-h-long assimilation window and then 21-h forward forecast (valid for 00 UTC of 30 October 2006).

5 Results and discussion

It is worth to mention at the beginning that in Figures latitude/longitude grid lines are plotted at two degree interval and center of the domain is lat. 13° N/long. 80° E (Chennai). The numbers written along *x* and *y* axis are distance in kilometer measured from left below corner in each diagram.

In order to investigate the impact of DWR observations in the analysis and forecasts of reflectivity (dBZ) at 850 hPa, as an overview, we present a comparison of the simulated reflectivity fields from control run, dwr_ad, and dwr_3d experiments (valid at 0300 UTC, 0600 UTC, 0900 UTC AND 1200 UTC) in Figs. 7, 8, 9, 10. Figures 7a, 8a, 9a, and 10a represents simulated reflectivity in dwr_ad experiment. Figures 7b, 8b, 9b, and 10b represents simulated reflectivity in dwr_3d experiment. Figures 7c, 8c, 9c, and 10c represents simulated reflectivity in control run experiment. In all the experiments, simulated reflectivity is compared with observed reflectivity, which is plotted in Figs. 7d, 8d, 9d, and 10d. Scale for Observed Reflectivity plots is given in Fig. 11.

Figure 7 shows analyzed reflectivity in all the experiments at 0300 UTC after 3-h-long assimilation cycles from 0000 UTC to 0300 UTC. Figure 7d depicts presence of two main cells in the observation, one is enclosed in circular region and other one is enclosed in elliptical region. Circular cell is approximately 150 km north of the center of the domain. Elliptical cell is approximately 200 km east of the center of the domain. These two cells are captured in dwr_ad and dwr_3d while in control run only extended pattern is seen.

In Figs. 8 and 9, forecast reflectivity fields of all the experiments are compared with the corresponding observations at 0600 UTC and 0900 UTC, respectively. The results show that the forecast reflectivity maintains spiral pattern both at 0600 UTC and at 0900UTC in circular area in the dwr_3d experiment. The northward movement of cyclone is captured realistically, but it crossed the land before the actual time of landfall. Reflectivity pattern in elliptical area is retained at 0600 UTC and 0900 UTC.

In Fig. 10, the forecast reflectivity fields (valid at 1200 UTC) in all these experiments show mismatch when compared with the corresponding observed fields. This is probably due to dominance of large-scale flow pattern.

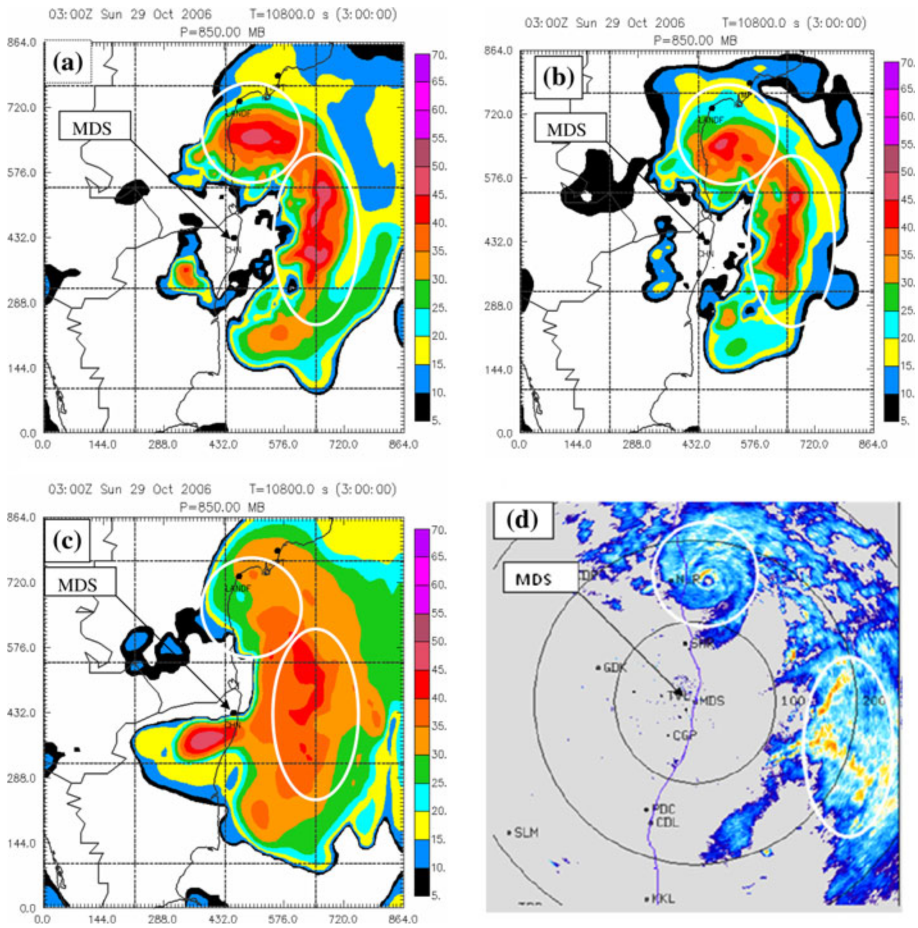

Fig. 7 Reflectivity plot at 0300 UTC. **a** dwr_ad experiment, **b** dwr_3d experiment, **c** control run experiment, **d** observed reflectivity by DWR station Chennai (MDS)

For quantitative comparison of the simulated storm intensity, the forecast reflectivity values of these experiments are compared with the corresponding observed maximum reflectivity. Table 2 presents inter-comparison between forecast reflectivity and the corresponding observed values at 0300 UTC, 0600 UTC, and 0900 UTC, respectively. At 0300 UTC, maximum observed reflectivity in both circular cell and elliptical cell is in the range of 49.3–52.0 dBZ, and analyzed reflectivity in dwr_ad and dwr_3d experiments is of the order 45–50 dBZ. In dwr_3d experiment, spiral rain band pattern is closely matching with the observed reflectivity. At 0600 UTC, observed maximum reflectivity in circular area is increasing and in elliptical area is decreasing. While simulated reflectivity in dwr_ad and dwr_3d experiments is increasing in both the area but still closely resembles in circular area. At 0900 UTC, observed maximum reflectivity in circular area is decreasing and in elliptical area is increasing when compared to previous observation at 0300 UTC. While simulated reflectivity in both the experiments show decreasing trend, the result of dwr_3d experiment remained very close to corresponding observed value.

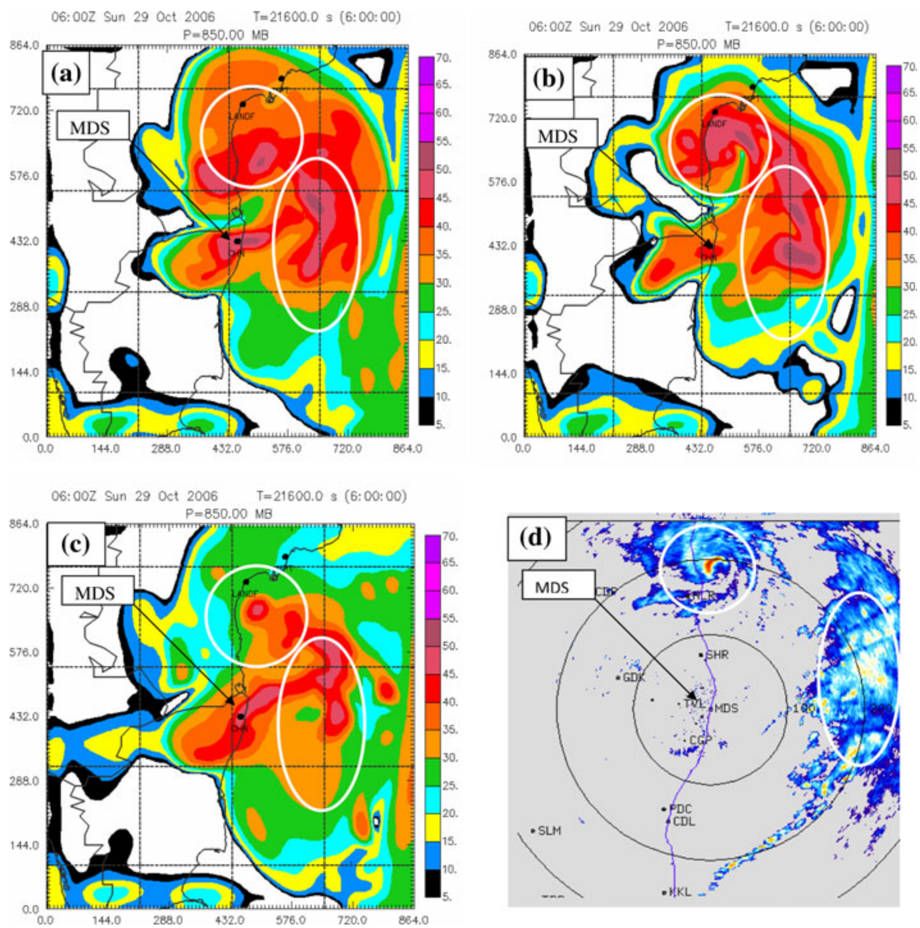

Fig. 8 Reflectivity plot at 0600 UTC. **a** dwr_ad experiment, **b** dwr_3d experiment, **c** control run experiment, **d** observed reflectivity by DWR station Chennai (MDS)

It can be seen that both the dwr_ad and dwr_3d could simulate reflectivity pattern. The region of highest reflectivity in both experiments could maintain the intensity of reflectivity up to 9 h forecast. Thereafter the dwr_ad and dwr_3d simulation shows' weakening trend and hardly any difference is noticed in the reflectivity fields between the dwr_ad, dwr_3d, and control run at 1200 UTC hours forecast. Spiral rain band structure of cyclone is maintained more clearly in dwr_3d when compared to dwr_ad.

6 Concluding remarks

The main objective of this study was to make an inter-comparison of performance of ADAS and 3DVAR data assimilation technique for simulation of the Bay of Bengal small-scale cyclone Ogni of 29–30 October 2006 using radial wind and reflectivity observations of DWR Chennai (lat. 13.0° N and long. 80.0° E) in the assimilation cycle of the storm

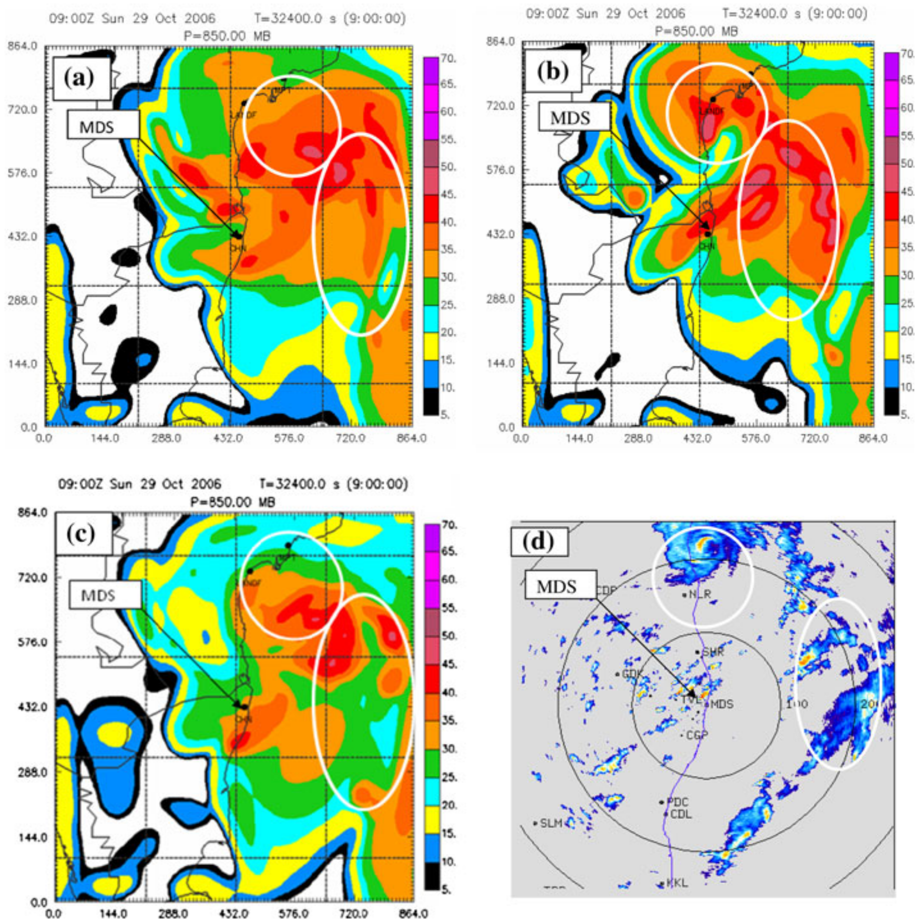

Fig. 9 Reflectivity plot at 0900 UTC. **a** dwr_ad experiment, **b** dwr_3d experiment, **c** control run experiment, **d** observed reflectivity by DWR station Chennai (MDS)

scale NWP system ARPS version (5.2.9) at the 9 km horizontal resolution. The results of the study shows that the model with the use of both ADAS and 3DVAR and ingesting DWR observations (Chennai) could simulate the small-size cyclonic storm in the analysis and forecasts. The model with DWR assimilation in both dwr_ad and dwr_3d run could retain the intensity of the cyclone up to 9 h of forecasts. Thereafter it shows weakening trend and underestimation of the intensity. Perhaps it arises due to the dominance of the large-scale characteristics over the local features present in the initial fields (NCEP GFS) with the progress of time integration and when the cyclone was drifting away to the north from the radar location.

The inter-comparison of results reveals that the experiment with the 3DVAR assimilation technique produces more realistic forecast to capture the genesis, structure, and northward movement of the cyclone in the short-range time scale. The 3DVAR technique includes a mass divergence constraint for coupling the wind components, which helps to produce better rotation field. Consequently, northward movement of the system and proper

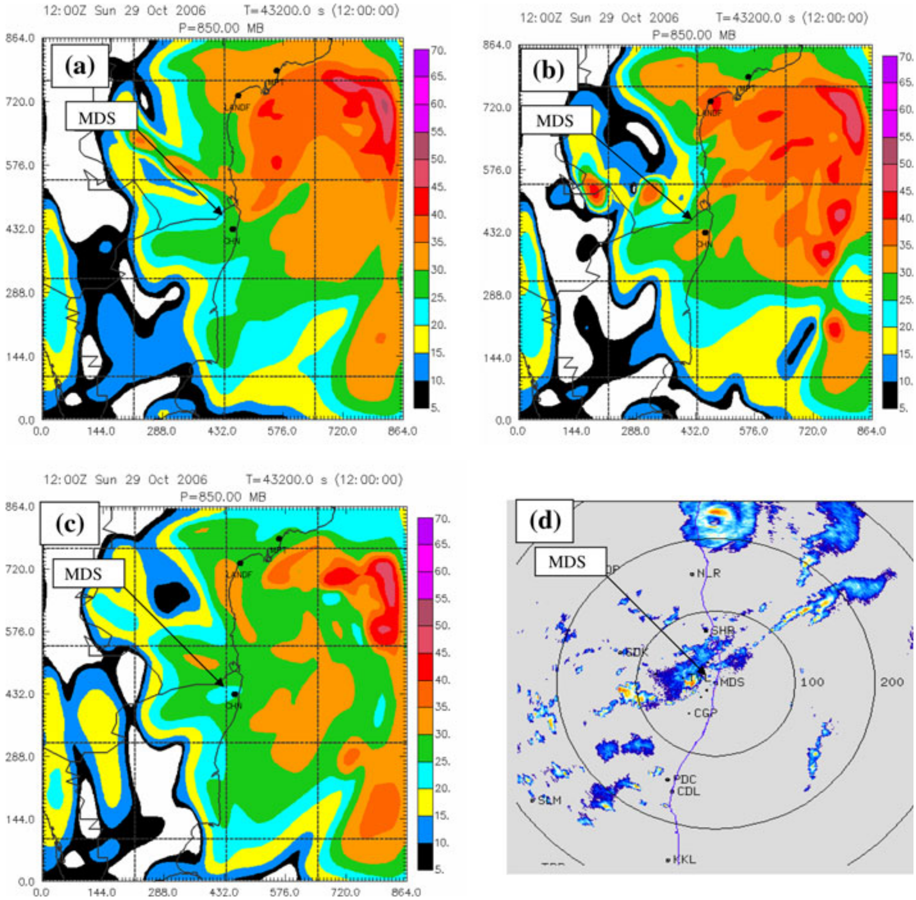

Fig. 10 Reflectivity plot at 1200 UTC. **a** dwr_ad experiment, **b** dwr_3d experiment, **c** control run experiment, **d** observed reflectivity by DWR station Chennai (MDS)

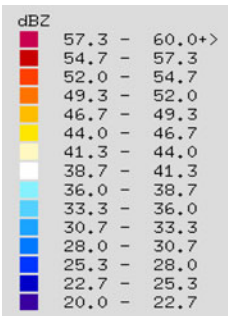

Fig. 11 Scale for observed reflectivity plots

spiral band structure was better captured in the 3DVAR experiment. The full advantage of 3DVAR scheme will be realized only when more indirect observations are involved and proper estimates of the back-ground and observational error correlations are used.

Table 2 Observed and predicted reflectivity (Maximum)

S. no.	Name of experiment	03 UTC		06 UTC		09 UTC	
		Circular area	Elliptical area	Circular area	Elliptical area	Circular area	Elliptical area
1	Control run	35–40	35–40	45–50	45–50	35–40	35–40
2	Dwr_ad	45–50	45–50	50–55	50–55	35–40	45–50
3	Dwr_3d	45–50	45–50	50–55	50–55	45–50	45–50
4	Observation	49.3–52.0	49.3–52.0	52.0–54.7	44.0–46.7	49.3–52.0	49.3–52.0

Acknowledgments The authors are thankful to Director General of Meteorology, India Meteorological Department (IMD) New Delhi and the Director of CAPS, at the University of Oklahoma for rendering all facilities to carry out this work. Authors like to convey their sincere thanks to the US Agency for International Development for kind approval of this Indo-USAID project. Authors are also thankful to anonymous reviewers who helped to improve the presentation of the paper.

References

Abhilash S, Das S, Kalsi SR, Gupta MD, Kumar KM, Geroge JP, Banerjee SK, Thampi SB, Pradhan D (2007) Assimilation of Doppler Weather Radar observations in the mesoscale model for the prediction of intense rainfall events associated with mesoscale convective systems using 3DVAR. J Earth Sys Sci 116(4):275–304

Albers SC, McGinley Birkenhuer DA, Smart JR (1996) The local analysis and prediction system (LAPS): analysis of clouds, precipitation and temperature. Wea Forecast 11:273–287

Bratseth AM (1986) Statistical interpolation by means of successive corrections. Tellus 38A:439–447

Brewster K (1996) Application of a Bratseth analysis scheme including Doppler radar data. Preprints 15th Conference on Wea Analysis and Forecasting. Am Meteor Soc 92–95

Brewster K (2002) Recent advances in the diabetic initialization of a non-hydrostatic numerical model. Preprints 21st conference on severe local storms and Preprints 15th conference on numerical weather prediction and 19th conference on weather analysis and forecasting, San Antonio, TX. Am Meteor Soc J 51–54

Brewster K, Shapiro A, Gao J, Kemp EM, Robinson P, Thomas KW (2003) Assimilation of radar data for the detection of aviation weather hazards. Preprints 31st conference on radar meteorology, Seattle, WA. Am Meteor Soc, Boston 118–121

Gao J, Xue M, Brewster K, Carr F, Droegemeier KK (2002) New development of a 3DVAR system for a non-hydrostatic NWP model. Preprints 15th conference on numerical weather prediction and 19th conference on weather analysis and forecasting, San Antonio, TX. Am Meteor Soc 339–341

Gao J, Xue M, Brewster K, Droegemeier KK (2004) A three-dimensional variational data analysis method with recursive filter for Doppler radars. J Atmos Ocean Tech 21:457–469

Hatwar HR, Subrahmanyam V, Mohapatra M, Roy Bhowmik SK, Bandyopadhay BK, Singh C, Srivastava K (2008) A report on the cyclonic storm OGNI of 2006. IMD Met Monograph No: Cyclone Warning Division 2/2008

Hu M, Xue M, Gao JD, Brewster K (2005a) 3DVAR and cloud analysis with WSR-88D Level-II data for the prediction of Fort Worth Tornadic thunderstorms part I: cloud analysis. Mon Wea Rev 134(2):675–698

Hu M, Xue M, Gao JD, Brewster K (2005b) 3DVAR and cloud analysis with WSR-88D level-II data for the prediction of Fort Worth Tornadic thunderstorms part II: impact of radial velocity analysis via 3DVAR. Mon Wea Rev 134(2):699–721

Lakshmanan V, Smith T, Stumpf G, Hondi KD (2006) The warning decision support system integrated information. Weather Forecast 22:596–612

Sen Roy S, Lakshmanan V, Roy Bhowmik SK, Thampi SB (2010) Doppler weather radar based nowcasting of cyclone Ogni. J Earth Sys Sci 119(2):183–199

Srivastava K, Roy Bhowmik SK, Sen Roy S, Thampi SB, Reddy YK (2010) Simulation of high impact convective events over Indian region by ARPS model with assimilation of Doppler weather radar radial velocity and reflectivity. Atmofera 23(1):53–73

Waldteufel P, Corbin H (1979) On the analysis of single Doppler radar data. J Appl Meteorl 18:532–542
Xue M, Wang D, Gao J, Brewster K, Droegemeier K (2003) The advanced regional prediction system (ARPS), storm scale numerical weather prediction and data assimilation. Meteor Atmos Phy 82:139–170
Zhang J, Carr F, Brewster K (1998) ADAS cloud analysis. Preprints 12th conference on numerical weather prediction, Phoenix, AZ. Am Meteor Soc Boston 185–188